Article

Alive and dead earthworms capture carbon during mineral weathering through different pathways

Check for updates

Tullia Calogiuri [1,2] ✉, Mathilde Hagens [2], Jan Willem Van Groenigen[1], Florian Wichern [3], Reinaldy P. Poetra[4], Lukas Rieder[4], Ivan A. Janssens [5], Jens Hartmann[4], Anna Neubeck [6], Harun Niron[7], Abhijeet Singh[6,8], Siegfried E. Vlaeminck [7], Sara Vicca [7] & Alix Vidal[1]

Enhanced rock weathering aims at capturing atmospheric carbon dioxide as inorganic carbon, while potentially stabilizing soil organic carbon. However, the role of soil biota in this process remains underexplored. Earthworms, being key soil engineers, may impact carbon dynamics both when alive, through mineral ingestion and casting activities, and when dead, through microbial processes. Using stable isotope tracing, we investigate how live and dead earthworms affect carbon dynamics during rock weathering. We demonstrate that both living and dead earthworms contributed to carbon capture, albeit through distinct pathways. Live earthworms enhanced the formation of organo-mineral associations via their dejections over time, promoting organic carbon persistence. Dead earthworms boosted microbial abundance and activity, enhancing organo-mineral associations and atmospheric-derived inorganic carbon capture between 60 and 120 days. We show that earthworms influence carbon cycling beyond their lifespan, with contrasting physico-chemical and biological pathways driving carbon capture through rock weathering throughout their life cycle.

Understanding and enhancing the pathways behind soil carbon (C) capture and stabilisation is crucial to limiting global temperature increases to 1.5 °C[1]. Effectively lowering atmospheric carbon dioxide (CO_2) concentrations requires multiple Carbon Dioxide Removal (CDR) technologies[2,3]. Among them, Enhanced Rock Weathering (ERW) is emerging as a promising CDR technology[4,5] aimed at capturing atmospheric CO_2 in the form of inorganic carbon (IC). ERW relies on the natural process of mineral weathering occurring in soils[3,6], where minerals react with CO_2 dissolved in soil water[4], releasing cations such as calcium (Ca) and magnesium (Mg), and generating IC in the form of carbonate and bicarbonate anions[7]. This dissolved inorganic carbon (DIC) can either reprecipitate as soil inorganic carbon (SIC) or leach to oceans through groundwater and waterways where it can be stored for thousands to millions of years[7]. While much ERW research so far has focused on enhancing IC capture through the addition of finely ground, fast-weathering silicate minerals to soils[5], its potential for soil organic matter (SOM) and further organic carbon (OC) stabilisation has been largely overlooked[7,8]. Secondary minerals formed during weathering can lead to the formation of mineral-associated organic matter (MAOM), regarded as the

most persistent SOM pool[7,9] compared to more labile ones as particulate organic matter (POM)[10]. However, studies investigating the synergies between IC capture and OC stabilisation through weathering remain limited[7], especially when considering biotic drivers of these processes[11,12].

Among the most promising biotic drivers of ERW are earthworms[12,13]. Earthworms are prominent soil ecosystem engineers that drive key soil functions by shaping soil structure and microbial communities, and thus biogeochemical cycles. More specifically, they play a notable role in C dynamics and may increase OC stabilisation[14]. During the ingestion of soil, mineral particles are ground in the gizzard of earthworms, which increases their available surface area[15] and exposes them to further attack by microbes living in earthworm intestines[16–19]. Once egested, mineral particles are thus smaller[20] and possess higher adsorption capacities[21], which can result in the binding of OC and increased MAOM formation[20].

While most earthworm research focuses on their effect on OC dynamics and persistence, the above-mentioned processes may also enhance mineral weathering rates and thus IC capture, a process that has received little attention so far. The ingestion and grinding of mineral

---

[1]Soil Biology Group, Wageningen University & Research, Wageningen, The Netherlands. [2]Soil Chemistry Group, Wageningen University & Research, Wageningen, The Netherlands. [3]Sustainable Food Systems Research Centre, Rhine-Waal University of Applied Sciences, Kleve, Germany. [4]Institute for Geology, Uni Hamburg, MIN, Hamburg, Germany. [5]Centre of Excellence PLECO (Plants and Ecosystems), University of Antwerp, Wilrijk, Belgium. [6]Department of Earth Sciences, Uppsala University, Uppsala, Sweden. [7]Biobased Sustainability Engineering (SUSTAIN), University of Antwerp, Antwerpen, Belgium. [8]Faculty of Agriculture, Allied Sciences and Technology, Ganpat University, Mehsana, India. ✉e-mail: tullia.calogiuri@wur.nl

particles[15] and their inoculation with microbes[19,22] and mucus rich in organic acids and enzymes[17] can further increase weathering by reducing particle size and altering its composition. Besides, earthworms might stimulate mineral dissolution by enhancing the activity of microbes living in the surrounding soil[23] and through bioturbation[23], which fosters the mixing of mineral particles and influences water flow, factors known to stimulate weathering. Gaining a comprehensive understanding of the role of earthworms in C cycling requires considering their dual effects on MAOM and IC formation through mineral weathering.

Another important yet rarely considered aspect in earthworm research is their high mortality rates in natural and experimental settings[24]. Decomposing earthworm bodies provide an immediately available pool of C and nutrients[22–24], which may shape microbial community composition[25] and increase microbial biomass[26] even more strongly than when living. As living earthworms, dead earthworms may enhance mineral weathering, and thus OC stabilisation and IC capture but through microbially-driven pathways rather than physico-chemical ones[27,28]. Earthworm bodies' decomposition boosts microbial activity, which can accelerate OM breakdown and further CO_2 release[29], further enhancing carbonation weathering and contributing to the formation of DIC[30]. Additionally, a greater microbial activity can result in a higher release of organic acids, which enhances weathering by modifying the pH at the surface of the minerals[27]. The same microbially-mediated mechanisms through which dead earthworms might influence IC sequestration could enhance OC stabilisation in the form of MAOM. However, no study to date has experimentally determined the pathways through which dead earthworms influence C dynamics through mineral weathering compared to live ones.

Here, we conducted a 120-day column experiment to investigate the different pathways through which live and dead earthworms influence OC and IC dynamics through weathering. To capture the overlooked contribution of dead earthworms to C dynamics and trace the origin of C, we introduced both live and dead earthworms (see Section "Materials and Methods") of the model species *Aporrectodea caliginosa* [Savigny] in columns filled with silicate rock powder (basanite), together with ^{13}C-labelled plant litter (pea straw). We analysed ^{13}C in the leachate, as both OC and IC. The use of ^{13}C tracing in the leachate is a key innovation of this study, enabling us to determine the origin of the captured CO_2 in the form of DIC. Determining whether CO_2 was plant- or atmospheric-derived gives insights into whether atmospheric CO_2 is actually captured during mineral weathering. Additionally, to depict the effect of earthworms on OM formation and persistence, we monitored CO_2 emissions over time and quantified C in free particulate organic matter (fPOM), occluded particulate organic matter(-oPOM), and MAOM fractions. We also conducted a phospholipid fatty acid (PLFA) analysis to assess how live and dead earthworms affected microbial abundance and composition, and how these changes influenced carbon dynamics. Mineral weathering rates were assessed using total alkalinity and major cation concentrations as proxies. Results highlight strikingly distinct pathways through which live and dead earthworms contribute to OC stabilisation and IC capture via weathering. These findings underscore the particular important role that dead earthworms play in C dynamics through microbially mediated processes, and the relevance of considering the full life-cycle of soil organisms when assessing their contributions to these processes.

Results

Dead earthworms contribute to IC capture

To determine whether the C in the leachate was of plant origin or derived from other sources and influenced by earthworm presence, we used the measured isotopic signature to quantify the amount of litter-derived and non-litter derived C in both dissolved organic carbon (DOC) and DIC. No significant differences could be found between treatments after 60 days for either litter and non-litter derived C in DOC and DIC ($P > 0.05$, Fig. 1). After 120 days, treatments where earthworms were added dead led to significantly higher concentrations of DIC ($P = 0.05$, $F = 38.37$, df = 3; see Supplementary Fig. 4) and, in particularly, of non-litter derived C in DIC ($P = 0.04$, $F = 3.97$,

df = 2) and DOC ($P = 0.0002$, $F = 17.3$, df = 2) compared to treatments with only litter (Fig. 1). Earthworms added alive did not significantly enhance DIC compared to control treatments with only litter ($P > 0.05$). Additionally, we found that around 50% of DIC was litter-derived (55.41% for only litter treatments, 52.83% for live earthworm treatments and 51.38% for dead earthworm treatments), suggesting that the other half of the inorganic C in the leachate must have originated from a source other than CO_2 from plant litter decomposition (Fig. 1).

Besides, to evaluate the legacy effects of earthworms on weathering through commonly measured weathering indicators, we quantified total alkalinity, electrical conductivity (EC, $\mu S \cdot cm^{-1}$), pH expressed as [H^+], and calcium (Ca), magnesium (Mg), potassium (K), sodium (Na), silicon (Si), phosphorus (P) and iron (Fe) leached from the columns. Dead earthworms led to significantly higher Mg concentrations ($P = 0.02$, $F = 29.59$, df = 3) and EC ($P = 0.03$, $F = 43.1$, df = 3) and an increasing trend for Fe concentrations ($P = 0.06$, $F = 33.89$, df = 3) compared to only litter after 120 days (see Supplementary Fig. 4). No significant differences could be found for the other measured indicators between treatments at either sampling points, irrespective of whether concentrations, or total amounts ($P > 0.05$, see Supplementary Fig. 6), were considered. Time had an effect on concentrations, leading to lower concentrations over time because of higher dilution ($P < 0.05$), but did not have an effect on total amounts ($P > 0.05$), except for live earthworm treatments where Ca amounts increased over time ($P = 0.01$, $F = 14.61$, df = 7) and an increasing trend could be detected for DIC ($P = 0.089$, $F = 14.68$, df = 3) and Mg ($P = 0.061$, $F = 43.01$, df = 7) (See Supplementary Fig. 5).

### Earthworms impact temporal MAOM-C dynamics

We assessed how earthworms affected C stabilisation in the organo-mineral mixture by analysing C contents in different OM fractions separated through density fractionation. Earthworms were found to influence MAOM-C dynamics over time, as both live and dead earthworms led to a higher accumulation of MAOM-C from 60 to 120 days ($P = 0.034$, $F = 11.53$, df = 7 and $P = 0.030$, $F = 11.53$, df = 7, respectively), with an average 42.86% and 22.22% increase, respectively (Fig. 2). However, despite these increases, the effect of earthworms on the allocation of C in the MAOM fraction was not significantly different from the control with only litter at either sampling time ($P > 0.05$). Moreover, no differences in MAOM-C over time were found for treatments with only litter ($P > 0.05$). No SIC formed in the MAOM fraction in either of the treatments as values measured in samples burned at 550 °C to remove organic carbon were not detected.

Over time, concentrations of fPOM-C decreased in treatments with either live or dead earthworms ($P = 0.013$, $F = 11.30$, df = 3, $P = 0.0068$, $F = 11.30$, df = 3), while no such changes were observed in only litter treatments (Supplementary Fig. 6). Concentrations of C in the oPOM fraction showed no significant differences across treatments or sampling times ($P > 0.05$; Supplementary Fig. 6). The treatments with only rock were always significantly different from the other treatments for all three fractions. No fPOM and oPOM fractions were extracted in this treatment, and the C measured in the MAOM fraction was equal to 0 mg·g⁻¹ organo-mineral mixture.

Microbial abundance is boosted by dead earthworms

To determine the effect of earthworms on microbial community composition, we investigated the total microbial biomass, bacteria, fungi, gram positive (GP) and gram negative (GN) bacteria abundance and gram positive:gram negative (GP:GN) and fungal:bacterial ratios. After 120 days, we found higher total microbial, bacterial and fungal abundances in dead earthworms compared to live earthworms and only litter treatments ($P < 0.05$; Table 1, Fig. 3), while we could not detect a significant difference in either ratio between treatments ($P > 0.05$; Table 1). The higher bacterial abundance in dead earthworm treatments was mainly driven by GN bacteria, which PLFA concentrations were 18% and 22% higher compared to live earthworm and only litter treatments, respectively (Fig. 3), while no

Fig. 1 | Litter and non-litter derived dissolved carbon (C) according to treatment and sampling time. Litter and non-litter derived C concentrations in dissolved organic carbon (DOC) and dissolved inorganic carbon (DIC) are shown after 60 and 120 days in panel a and panel b, respectively, according to different treatments. Values are expressed in mg·L^{-1}. Values represent the mean for five independent replicates. Asterisks indicate significant differences between treatments ($P < 0.05$). Statistical significance was analysed using ANOVA followed by a post hoc Tukey's test. BP = treatment with basanite and pea straw; BPEa = treatment with basanite, pea straw and earthworms added alive; BPEd = treatment with basanite, pea straw and earthworms added dead.
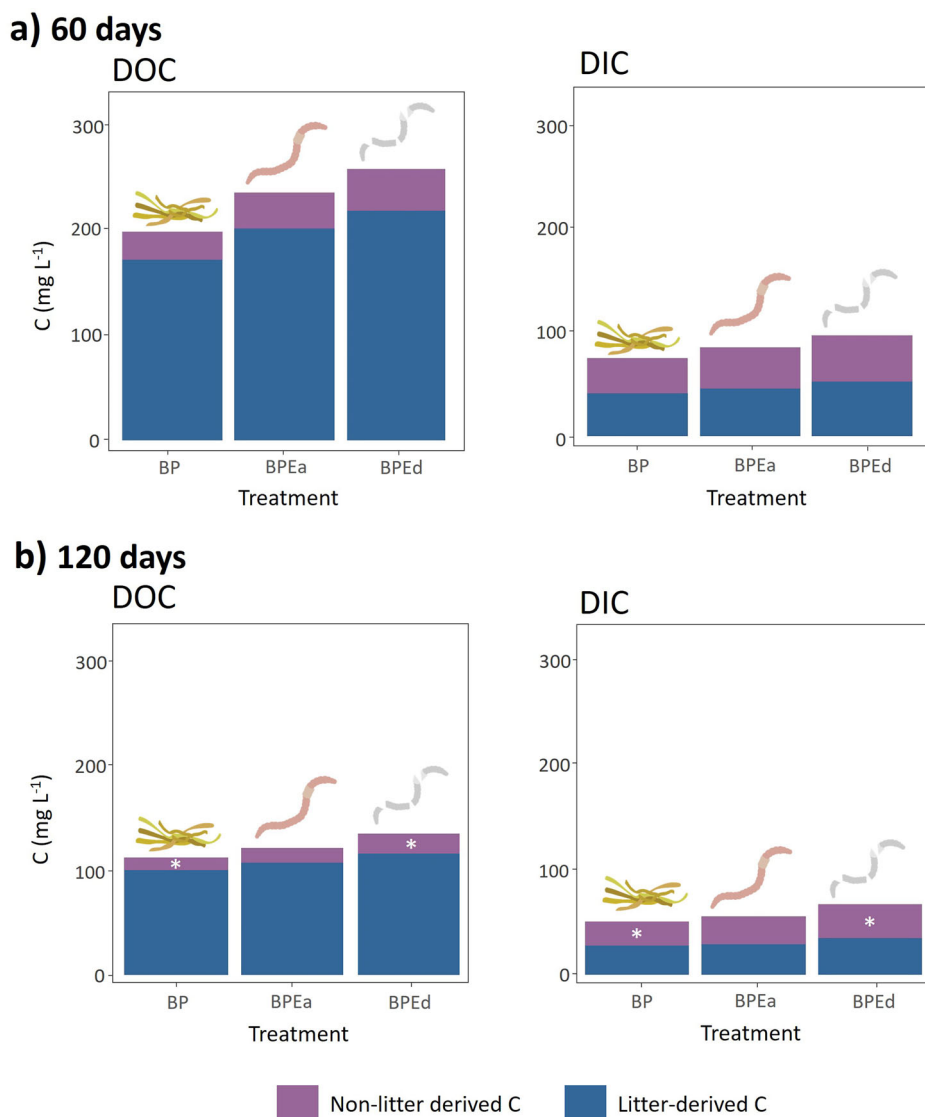
significant differences were found for GP bacteria abundance between treatments ($P > 0.05$; Fig. 3). Treatments with only rock were always significantly different ($P < 0.05$) from other treatments as values for both bacterial and fungal biomass were below detection limit.

Dead earthworms result in highest respiration rates

To trace the effects of live and dead earthworms on C cycling, CO_2 emissions were measured throughout the 120 days of incubation and the cumulative CO_2-C emitted by the end of the experimental period was calculated for each treatment. Dead earthworms emitted significantly more CO_2-C compared with only litter ($P < 0.05$), whereas live earthworms did not significantly affect CO_2 emissions ($P > 0.05$) (Fig. 4). Rock-only treatments neither emitted nor consumed CO_2-C throughout the experimental period, therefore, total cumulative emissions were significantly different from all other treatments ($P < 0.05$).

Discussion

Our results shed light on the pathways through which earthworms contribute to IC capture and OC stabilisation across their entire life cycle. The effect of earthworms, both introduced alive and dead, on IC capture is depicted through weathering indicators, including the DIC quantified in the water that flew through the mineral mixture, i.e. the leachate. After four months, dead earthworms increased the capture of CO_2 derived from the

atmosphere through mineral weathering, as reflected by the higher non-litter derived C in DIC (Fig. 1) and Mg concentrations and EC, as well as increasing trend in Fe (see Supplementary Fig. 4), common weathering indicators[31], within the leachate. The abundant bacterial community depicted in the presence of dead earthworms (Table 1; Fig. 3) may have enhanced mineral dissolution rates by producing organic acids and chelates to access nutrients, which lower the pH and decrease ion concentrations at the mineral surface[12,27]. Besides, a higher microbial abundance translates into higher microbial respiration, as shown by our CO_2 emission data. The resulting increase in CO_2 concentration might have increased carbonic acid concentrations and mineral weathering, producing bicarbonate that leach out of the organo-mineral mixture as DIC[30].

Earthworms introduced alive also influenced DIC through weathering, but to a lesser extent compared to dead earthworms (see Supplementary Fig. 5). Live earthworms did not increase any weathering indicator compared to the control with only litter, but over time they did increase significantly total Ca, and marginally total DIC and Mg (see Supplementary Fig. 5). We suggest that this process may have begun in fresh casts, which are known to be rich in microbes[32] that affect weathering through their activity, which is known to decrease in ageing cast[32,33]. It has to be noted that the litter was enriched with pulse labelling, so we cannot exclude that part of the non-labelled DIC was originating from litter decomposition, while we can exclude it would have been derived by earthworms. Earthworms added

Fig. 2 | Carbon (C) content in mineral associated organic matter (MAOM) according to treatment and sampling time. Values are expressed as mg C·g⁻¹ organo-mineral mixture. Values represent the mean and the bars the standard error for four independent replicates. Different letters indicate significant differences between treatments ($P < 0.05$). Statistical significance was analysed using ANOVA followed by a post hoc Tukey's test. B1 = treatment with basanite after 60 days; B2= treatment with basanite after 120 days; BP1 = treatment with basanite and pea straw after 60 days, BP2= treatment with basanite and pea straw after 120 days; BPEa1 = treatment with basanite, pea straw and earthworms added alive after 60 days; BPEa2= treatment with basanite, pea straw and earthworms added alive after 120 days; BPEd1 = treatment with basanite, pea straw and earthworms added dead after 60 days; BPEd2= treatment with basanite, pea straw and earthworms added dead after 120 days.
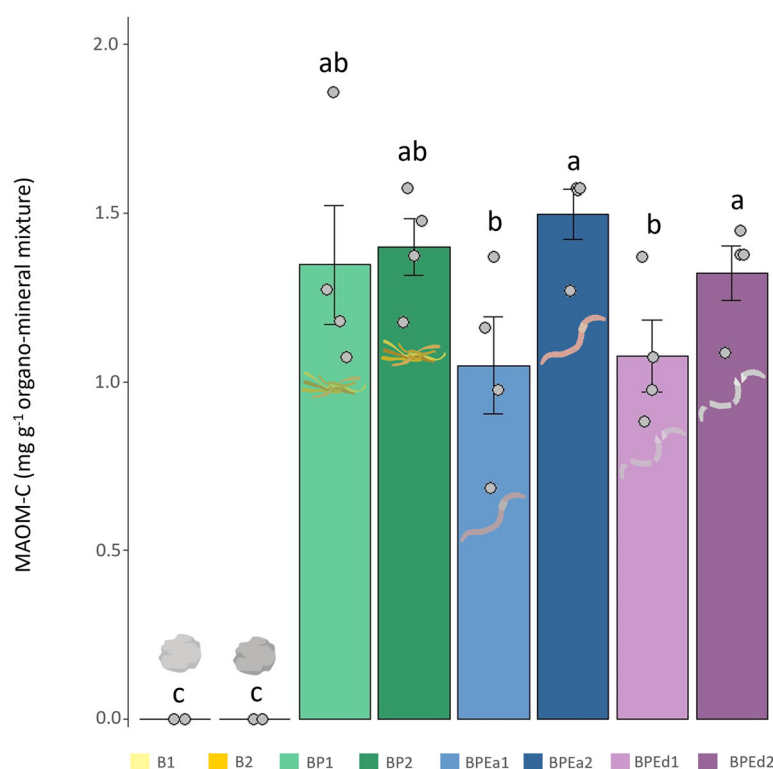
either alive or dead contained very little C (see Supplementary Fig. 3) resulting to be negligible compared to the total DIC.

Earthworms have a double-edged sword effect on OC stabilisation, simultaneously promoting carbon losses through biological respiration and enhancing carbon stabilisation through protection mechanisms[14,34,35]. As a result, earthworms had no net effect on OC stabilisation compared to a system with only litter and no earthworms (Fig. 2). Yet, we highlight an increase with time of OC in MAOM, the most persistent SOM pool[7,9], in the presence of earthworms. Therefore, we highlight contrasting pathways through which both live and dead earthworms influence OC stabilisation by gradually increasing the C content in the MAOM fraction (Fig. 2). The formation of MAOM is enhanced by living earthworms that feed on the mineral mixture, which is further processed within their intestines, changing its chemical and physical characteristics once egested as casts[17]. After being grinded in earthworm gizzards, mineral particles are thus smaller[20] and possess higher adsorption capacities[21]. As a result, this process notably enhances the formation of new mineral surfaces[20], facilitating the protection and thus the stabilisation of OC over time[20]. This may be driven by physical mechanisms, such as the formation of stronger linkages between clay and OM, and chemical mechanisms, including increased thermal stability and oxidation of OM, which enhances its adsorption onto mineral surfaces[14]. Notably, this increase in MAOM was accompanied by a decrease in fPOM, while oPOM remained relatively unchanged (Fig. 2, Supplementary Fig. 6). This likely results from the direct adsorption of labile C from litter onto reactive mineral surfaces[34] rather than microbial byproducts and necromass, as microbial biomass was comparable to the control (Fig. 3). The fine particle size and altered mineral properties of ageing casts enhance these interactions, enabling the direct transformation of fPOM into MAOM over being physically protected in aggregates as oPOM, resulting in the translocation of C to a more stable pool. The progressive stabilisation of C was further reflected in the limited C mineralisation, as depicted by the cumulative CO_2 emissions (Fig. 4) and the microbial abundance (Fig. 3), which remained comparable to the control containing only litter. While live earthworms are known for increasing microbial abundance due to their

casting activities, creating hotspots of nutrients[36], ageing casts contain more stable C forms and less microbes[20,37], as also shown by our PLFA results. We therefore highlight that ageing casts play a prominent role in driving OC stabilisation in the early stages of MAOM formation, through physical and chemical mechanisms, via mineral weathering. While our findings elucidate pathways through which ageing casts contribute to OC stabilization via mineral weathering, a key limitation lies in the inability to fully disentangle the effects of cast ageing from those arising from the decomposition of earthworm bodies, as all live earthworms died within the initial two months of the experiment (see Section "Materials and Methods"). Nonetheless, unlike previous studies that replaced earthworms upon death[34,38], isolated fresh casts[39,40] or removed them and let them age separately from the original system[41], our study left the system intact. This design enables a more integrated assessment of cast ageing processes and their contribution to soil carbon dynamics under more realistic, undisturbed conditions.

Contrary to earthworms added alive, dead earthworms enhanced microbial activity and abundance, especially bacterial abundance, as shown by our PLFA (Table 1, Fig. 3) and CO_2 emission (Fig. 4) results, respectively. Decomposing earthworm bodies liberate a pool of immediately available C and nutrients that serve as substrate for microbial growth[26], particularly for the bacteria[42,43] predominant in the presence of dead earthworms (Table 1, Fig. 3). Therefore, the stimulation of microbial communities may further explain the increase in the allocation of C in MAOM over time in the presence of dead earthworms (Fig. 2). Bacteria increase the production of extra-polymeric substances (EPS) to stick on mineral surfaces, which may serve as a gluing agent for MAOM formation[44]. Besides the exudation of EPS, microbes produce organic acids and chelates[27] to access nutrients from mineral particles. The release of these substances can modify the pH at the mineral surface and chelate ions away from the solution where minerals are reacting[44]. These processes can further alter mineral chemical and physical properties[45], leading to an increase in MAOM. A higher microbial abundance can also lead to a higher microbial necromass, which can substantially contribute to MAOM formation[46,47]. Similar as for the live earthworm treatment, also dead earthworms led to a direct translocation of fPOM into

MAOM while leaving oPOM unchanged (Fig. 2, Supplementary Fig. 6). For dead earthworms, the higher microbial biomass (Fig. 3) accelerates fPOM degradation, releases microbial byproducts and enhances microbial necromass. These compounds are highly sorptive and bind directly to the altered mineral surfaces[48,49], bypassing oPOM formation through aggregation while leading to the development of MAOM. Our results suggest that dead earthworms primarily drive OC stabilisation processes through biological mechanisms enhancing MAOM formation, in contrast to the dominant physical and chemical mechanisms associated with earthworms added alive.

Our results emphasize the importance of considering the entire life cycle of soil organisms when investigating their effect on biogeochemical cycles. We demonstrate that alive and dead earthworms contribute to OC stabilisation through different pathways during weathering, mainly driven by physico-chemical and biological mechanisms, respectively (Fig. 5). Besides, our results highlight the role of dead earthworm in IC capture, a process that has been largely overlooked but may be critical on a larger scale considering that earthworm biomass can turnover up to four times a year[50].

Materials and methods

Materials characteristics and experimental setup

A column experiment was carried out in an incubator at 20 °C for 120 days. We had four treatments: (i) only basanite as a technical control (B); (ii) basanite mixed with ^{13}C and ^{15}N enriched pea straw (BP); (iii) basanite mixed with ^{13}C and ^{15}N enriched pea straw and earthworms introduced alive (BPEa); (iv) basanite mixed with ^{13}C and ^{15}N enriched pea straw and earthworms introduced dead (BPEd). Each treatment was replicated 10 times. Five replicates were destructively sampled after 60 days (T1) and the other five replicates after 120 days (T2). As earthworms introduced alive died within 60 days, for simplification purposes we refer to treatment BPEa as alive earthworms treatment because the organo-mineral mixture was processed by earthworms (see section "Alive and dead earthworms"), therefore making it a different system compared to the dead earthworms treatment.

For this experiment, we used basanite (RPBL, Germany), a rock powder mainly composed of relatively fast-weathering silicate minerals[51] and containing very low initial carbon (C) (Table 2). Rock powder samples were analysed for their initial total C and N contents (FlashSmart, Thermo Fisher Scientific, USA) (Table 2). As initial C was below the detection limit of $0.1 \text{ mg} \cdot \text{g}^{-1}$, further analyses to quantify initial organic and inorganic C were

Table 1 | Total bacterial biomass, gram positive:gram negative (GP:GN) and fungal:bacterial ratios according to treatment after 120-day incubation. Biomass is expressed in picomol·kg^{-1}

Treatment	Total PLFA abundance (picomol·kg^{-1})	GP:GN ratio	Fungal PLFA:bacterial PLFA ratio
B	n.d.	-	-
BP	17,935 ± 752.7^b	0.8 ± 0.02^a	0.1 ± 0.01^a
BPEa	17,585 ± 754.4^b	0.8 ± 0.04^a	0.1 ± 0.01^a
BPEd	20,659 ± 312.8^a	0.7 ± 0.04^a	0.1 ± 0.01^a

Values indicate the mean and the bars the standard error for five independent replicates. Different italic superscript letters indicate statistically significant differences between treatments ($P < 0.05$). Statistical significance was analysed using a Kruskal–Wallis test followed by a post-hoc Dunn test. B= treatment with basanite; BP = treatment with basanite and pea straw; BPEa = treatment with basanite, pea straw and earthworms added alive; BPEd = treatment with basanite, pea straw and earthworms added dead. N.d. = not detectable.
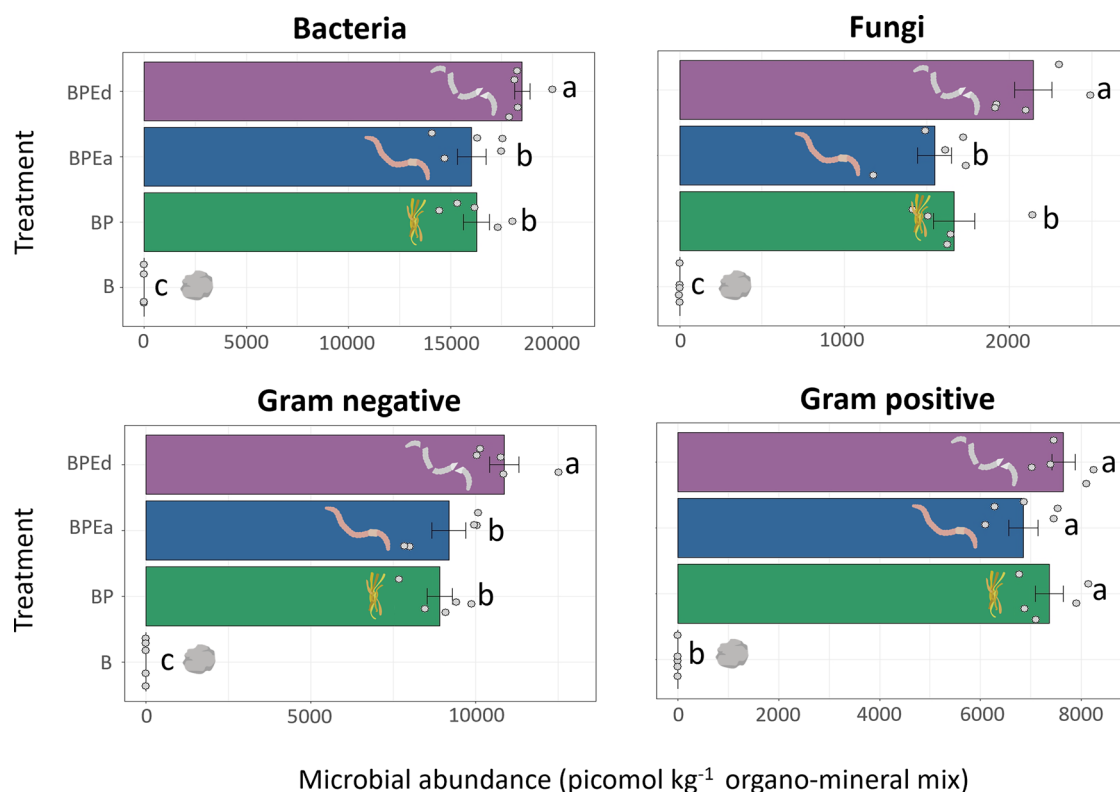

Fig. 3 | Group specific PLFA abundance according to treatment after 120-day incubation. Concentrations are expressed in picomol·kg^{-1} organo-mineral mixture. Values indicate the mean and the bars the standard error for five independent replicates. Different letters indicate significant differences between treatments ($P < 0.05$). Statistical significance was analysed using a Kruskal–Wallis test followed by a post-hoc Dunn test. B = treatment with basanite; BP = treatment with basanite and pea straw; BPEa = treatment with basanite, pea straw and earthworms added alive; BPEd = treatment with basanite, pea straw and earthworms added dead.
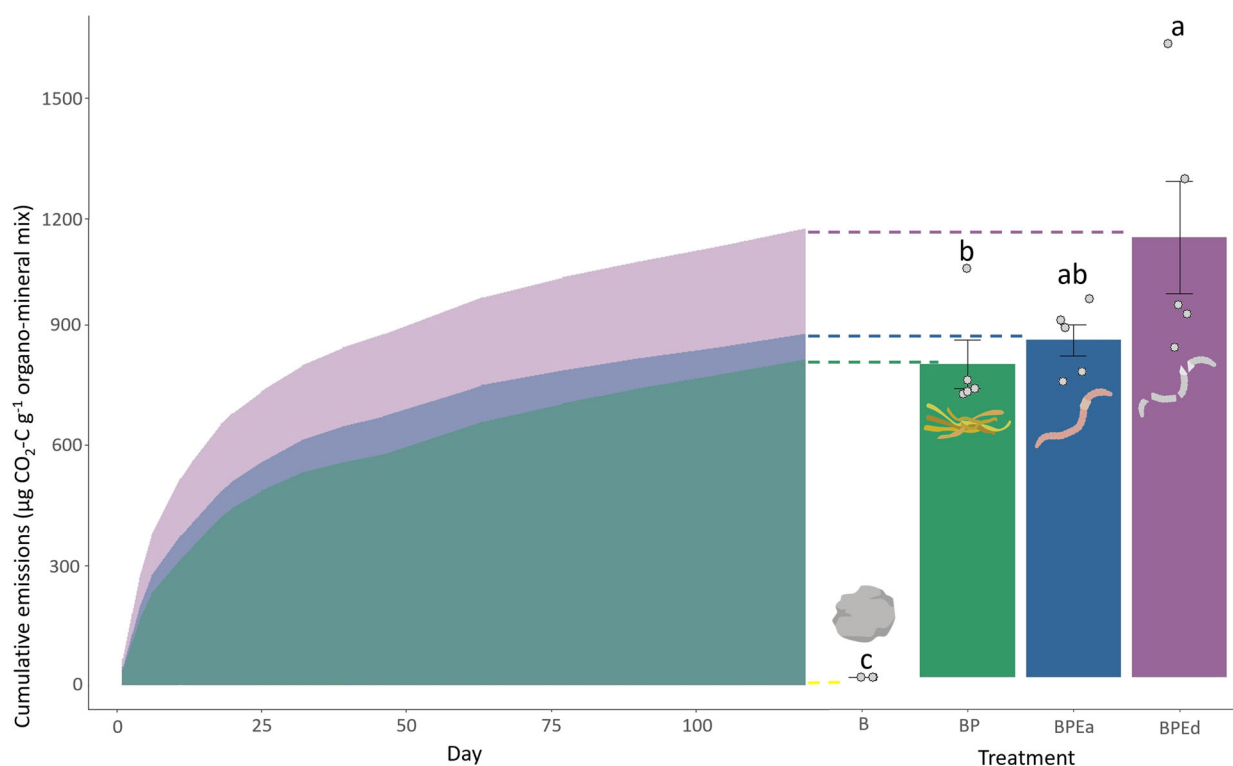
Fig. 4 | Respired CO$_2$-C during the 120-day incubation according to treatment. The trend of the cumulative and the total respired CO$_2$-C per treatment is shown on the left and on the right side, respectively. Values are expressed as CO$_2$-C µg·g^{-1} organo-mineral mixture. Values indicate the mean and the bars the standard error for five independent replicates. Different letters indicate significant differences between treatments ($P < 0.05$). Statistical significance was analysed using a Kruskal–Wallis test followed by a post-hoc Dunn test. B = treatment with basanite; BP = treatment with basanite and pea straw; BPEa = treatment with basanite, pea straw and earthworms added alive; BPEd = treatment with basanite, pea straw and earthworms added dead.

not carried out. The initial elemental composition of the rock was determined through X-ray fluorescence (Panalytical Magix Pro) (Table 2). The particle size distribution (PSD) was determined through laser diffraction (particle-sizer Sympathec HELOS/KF Magic) (see Supplementary Fig. 1). To facilitate drainage of the columns and further earthworms' survival and activity[28], we mixed 70% of the coarse grain size with 30% of the fine grain size to reach a total of 400 g dry weight of rock powder per column.

^{13}C and ^{15}N enriched straw from pea (*Pisum sativum* L.) plants was added to the rock flour as food source for earthworms. Enrichment of pea straw was obtained through multiple pulses of a sterilised ^{13}C-glucose (99 atom%) and ^{15}N-urea (95 atom%) solution using the cotton wick method during the plant growing period (see Hupe et al.[52] for more details). Initial ^{13}C and ^{15}N and total C and N of the pea straw were determined though an Elementar vario MICRO cube elemental analyzer (Elementar Analy-sensysteme GmbH, Langenselbold, Germany) interfaced to a Sercon Europa 20-20 isotope ratio mass spectrometer (Sercon Ltd, Cheshire, United Kingdom) at the University of Davis in California (Table 3). The pea straw was homogenised and grinded with a laboratory blender and sieved to obtain fragments in the range of 0.5–2 mm size. The plant residues were then mixed with the rock powder at a dose of 25 g dry matter·kg^{-1} rock flour. Water was added to reach a gravimetric water content of 0.15 g·g^{-1}. Afterwards, earthworms were introduced into the mixture and the columns were filled to a density of 1.19 ± 0.05 for the technical control and 0.86 ± 0.03 g·cm^{-3} for the other treatments. Starting from day 1 of the experiment, we watered columns three times a week at 50 mL·day^{-1} using demineralised water. We opted for frequent watering, as watering is known to enhance weathering rates by increasing the physical degradation of the rocks and by preventing the solute concentrations of pore water reacting with the rocks to reach saturation[53,54].

Columns (7 cm diameter × 15 cm height) made from polyvinyl chloride were closed at the bottom with a double polyester (PES) mesh system of 20 and 10 µm and were filled with the organo-mineral mixture. Filled columns were then placed in the incubator on top of funnels according to a completely randomised design. Funnels were connected through tubes to a Styrofoam fridge where bottles to collect the leachate were kept at a temperature of 7 °C to prevent composition changes in the leachate, adapted from Calogiuri et al.[55].

Live and dead earthworms

The endogeic earthworm species *A. caliginosa* [Savigny] was selected for this study because of its high abundance in the Netherlands and its feeding habits, mainly feeding on soil particles and associated OM[56]. We expected this species to particularly enhance weathering rates and further C stabili-sation because of physical and chemical processes, and consequent changes, affecting rock grains once ingested in earthworm guts[15,17–19,57,58]. Adult earthworms were collected before the start of the experiment from the park De Blauwe Bergen in Wageningen, The Netherlands (51°58′51.8″N 5°39′38.0″E). Afterwards, they were placed to starve for two days to empty their guts and their weight was recorded following the paper-filter method[59]. According to treatment, earthworms were added to the organo-mineral mixture immediately after the starving period either live or dead. We decided to have not only treatments with live earthworms but also treat-ments with dead earthworms because our previous findings showed that dead earthworms might enhance weathering rates and influence C stability due to microbially-mediated processes[28]. To produce dead earthworms, earthworms were placed in a tube rinsed with CO$_2$ until they became inactive. The opening of the tube was then covered with a balloon filled with CO$_2$ and placed in a container with ice cubes for 1 h to ensure earthworms did not survive. We used this method instead of direct freezing to avoid
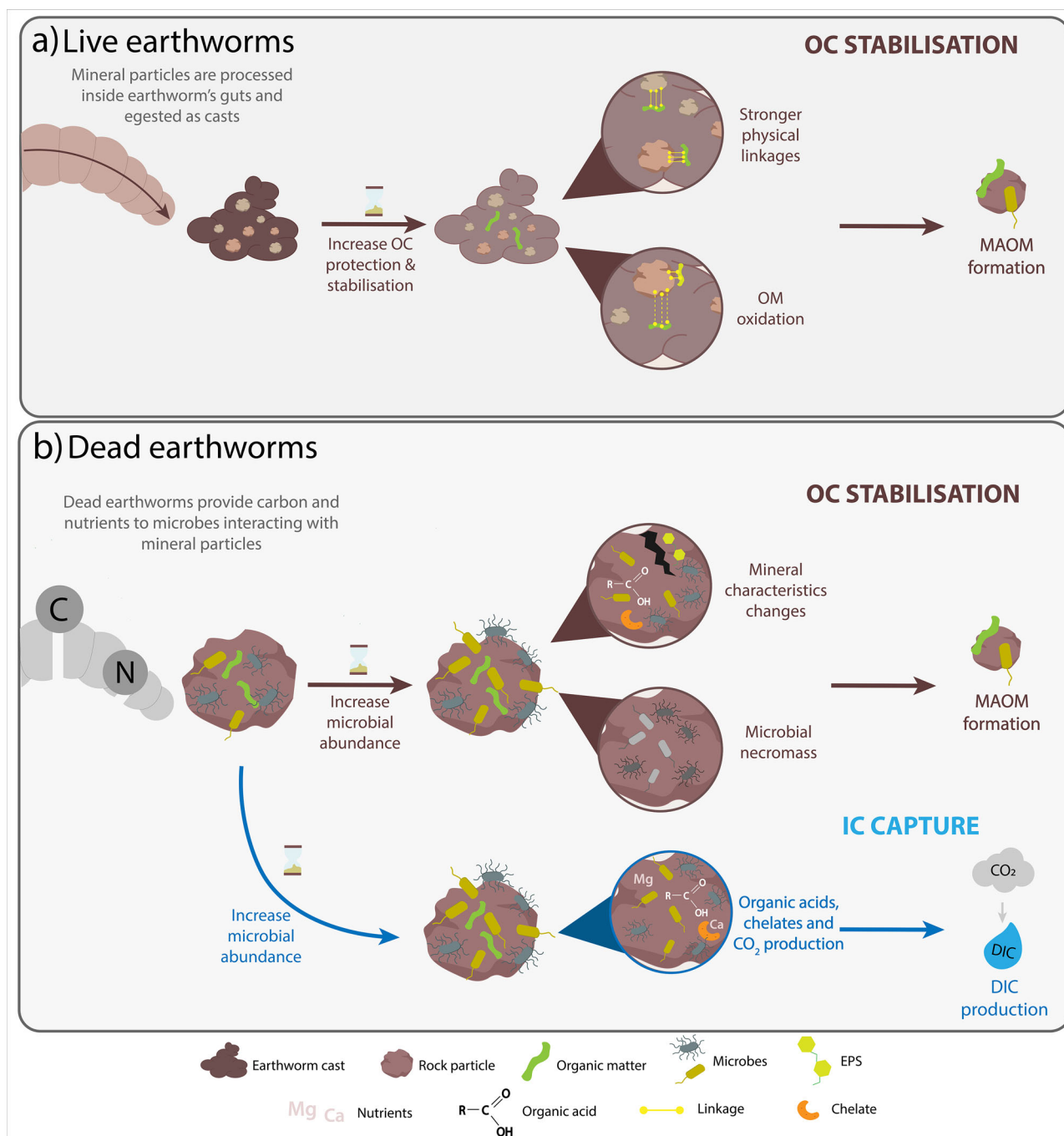
Fig. 5 | Pathways by which live and dead earthworms influence carbon dynamics. Schemativ overview of the contrasting pathways through which live (**a**) and dead (**b**) earthworms influence organic carbon (OC) stabilisation and inorganic carbon (IC) capture via mineral weathering. Live earthworms feed on mineral particles, which are processed within their intestines and egested finer and with higher adsorption capacities as casts. During casts ageing, OC is stabilised in the form of mineral-associated organic matter (MAOM) through the formation of stronger linkages between organic matter (OM) and mineral surfaces, as well as the progressive oxidation of OM. Dead earthworms provide an immediate pool of available carbon and nutrients for microbes in the mineral environment, boosting microbial abundance over time. This increase in microbial abundance enhances the production of extra-polymeric substances (EPS), to stick on mineral particles, and organic acids and chelates, to access nutrients, by microbes. These substances alter the characteristics of the mineral particles, favouring MAOM formation and further OC stabilisation. Besides, the higher microbial abundance can lead to higher microbial necromass, further contributing to MAOM. Additionally, the microbial-driven changes associated with dead earthworms also influence IC capture by accelerating mineral weathering through organic acid and chelates production, which enhances carbon dioxide (CO_2) capture as dissolved inorganic carbon (DIC). Brown and blue colours indicate mechanisms increasing OC stabilisation and IC capture, respectively.

disruption of earthworm tissues due to extreme cold and to obtain a more natural decomposition process afterwards. Earthworms were then added at 10 individuals·kg⁻¹ organo-mineral mixture and the average fresh weight per column was 0.85 ± 0.06 g. Afterwards, columns were covered with a mesh to prevent earthworms' escape. At both destructive sampling times, at 60 and 120 days, columns where earthworms were introduced live were sampled to

determine earthworm survival. Already at 60 days, no earthworm survived, but we could visually assess that earthworms were alive for a period long enough to process most of the organo-mineral mixture (see Supplementary Fig. 2). Visual assessment of casts production is generally used as an indicator of earthworm activity[60-62]. Therefore, we used BPEa treatments to investigate the effect of the ageing of earthworm-processed material on C

Table 2 | d10, d50 and d90 of the particle size distribution (PSD), carbon (C) and nitrogen (N) content, and elemental composition of basanite fine and coarse

Rock flour	d10	d50	d90	C	N	CaO	MgO	SiO$_2$	Fe$_2$O$_3$	Na$_2$O	K$_2$O	P$_2$O$_5$	Al$_2$O$_3$	TiO$_2$
Basanite: fine	0.008	0.035	0.073	b.d.l.	b.d.l.	12.6 ± 1	8.68 ± 0.12	43.44 ± 0.27	11.19 ± 0.26	2.99 ± 0.08	3.29 ± 0.09	0.53 ± 0.07	13.79 ± 0.25	2.58 ± 0.33
Basanite: coarse	0.924	1.536	1.340											

Values for d10, d50 and d90 are expressed in mm and values for elements are expressed as % oxides. Numbers represent mean and standard deviation for three replicates, except for the PSD where measurements were done for one replicate. B.d.l. = below detection limit, which was 0.1 mg g^{-1} for both C and N.

dynamics compared to BPEd treatments where the organo-mineral mixture had not been processed by earthworms.

Leachate isotope analyses and further characterisation

The leachate coming from the columns was filtered every two weeks over 0.45 μm and stored at 5 °C. At this point in time, samples were taken to measure pH and EC (mS·cm^{-1}) using a multi-parameter portable meter (WTW Multiline® Multi 2630 IDS). At both 60 and 120 days, the final weight of the leachate was recorded. Afterwards, a subsample of the leachate was frozen at −20 °C and then freeze-dried (Alpha 2-4 LSCbasic, serie nr 27630, Christ). The resulting powder was grinded, homogenised and 5 mg were weighed in either tin or silver cups. Samples in silver cups were acidified with 2 M HCl for 10 h and dried overnight at 60 °C to remove carbonates[20]. Non-acidified and acidified samples were then analysed for ^{13}C and ^{15}N through an Elementar vario MICRO cube elemental analyzer (Elementar Analysensysteme GmbH, Langenselbold, Germany) interfaced to a Sercon Europa 20-20 isotope ratio mass spectrometer (Sercon Ltd, Cheshire, United Kingdom) at the University of Davis in California. The ^{13}C values for IC were calculated using a mass balance according to the following equation adapted from De Troyer et al.[63]:

$$^{13}C_{IC}(atom \cdot \%) = \frac{^{13}C_{TC} \cdot TC - ^{13}C_{OC} \cdot OC}{IC} \tag{1}$$

where ^{13}C$_{TC}$ and ^{13}C$_{OC}$ are the atom% values while TC and OC are the concentrations in mg·g^{-1} measured in the leachate for total and OC, respectively. IC represents the concentration of inorganic C in mg·g^{-1}.

The proportion of litter-derived C (%) in the OC and IC measured in the leachate was then calculated as:

$$Litter - derived \cdot C(\%) = \frac{^{13}C_{labeled} - ^{13}C_{control}}{^{13}C_{litter} - ^{13}C_{control}} \tag{2}$$

Where ^{13}C$_{labeled}$ is the ^{13}C enrichment in the samples where labelled pea straw was added, ^{13}C$_{control}$ is the ^{13}C enrichment in controls where labelled pea straw was not added (natural abundance level 1.09 atom%) and ^{13}C$_{litter}$ is the ^{13}C enrichment of the added pea straw. All values are expressed in atom %. The litter-derived C in the OC and IC measured in the leachate was then determined as:

$$C_{litter}\left[mg\right] = \frac{litter - derived\ C}{100} x C_{leachate} x\, l\, w \tag{3}$$

Where $C_{leachate}$ is the amount of C measured as either OC or IC and lw is the weight of the leachate (g) collected at the end of the sampling points.

The remaining leachate was analysed for total dissolved carbon (TDC, mg·L^{-1}) and dissolved inorganic carbon (DIC, mg·L^{-1}) using an automated Segmented Flow Analyser (SFA) (Skalar, SAN^{++}). Dissolved organic carbon (DOC, mg·L^{-1}) was then calculated by difference. Leachate samples were also analysed for total alkalinity (mmol·L^{-1}) by titrating 5 mL of sample with 0.02 M HCl until reaching pH = 4.5. Besides, samples were also analysed for their concentrations of calcium (Ca, mg·L^{-1}), magnesium (Mg, mg·L^{-1}), potassium (K, mg·L^{-1}), sodium (Na, mg·L^{-1}), silicon (Si, mg·L^{-1}), phosphorus (P, mg·L^{-1}) and iron (Fe, mg·L^{-1}) through Inductively Coupled Plasma Optical Emission Spectroscopy (ICP-OES) (Thermo iCAP 6500 dual view), and pH and EC using a multi-parameter portable meter (WTW Multiline® Multi 2630 IDS). These variables were chosen as they are commonly used indicators to assess mineral weathering[5,64–67]. Concentrations of all the measured variables were also converted to total amounts using the final weight of leachate collected.

Organic matter fractionation and subsequent analyses

At the end of 60 and 120 days, around 9 g of dried samples from the organo-mineral mixture was collected using the coning and quartering method[68] to ensure the collection of homogeneous samples. Samples were then

Table 3 | Characterisation of the initial plant litter. Numbers represent the mean and standard deviation for ten replicates

	^{13}C (at-%)	^{15}N (at-%)	C (mg·g^{-1})	N (mg·g^{-1})	C:N
Pea straw	1.5 ± 0.1	3.9 ± 0.5	419.8 ± 5.2	18.0 ± 4.3	23.34

fractionated to separate fPOM, occluded organic matter (oPOM) and mineral associated organic matter (MAOM) using a density-based method adapted from Plaza et al.[69] and Cerli et al.[70]. Briefly, samples were saturated with 40 mL of Sodium Polytungstate (SPT, TC-Tungsten Compounds) solution with a density of 1.8 g·mL^{-1}. After centrifugation, the floating fPOM was collected using a vacuum filtration system and washed until EC was below 50 μS·cm^{-1} to remove excess SPT. The leftover sample was again saturated with SPT solution and sonicated by applying 60 J·mL^{-1} of energy through a sonicator (Sonics vibra-cell vcx130). Samples were then again centrifuged and the floating oPOM was collected and washed until conductivity was below 50 μS·cm^{-1} using a pressure filtration system. The remaining MAOM was then washed to remove excess SPT and centrifuged until EC was as well below 50 μS·cm^{-1}. All fPOM, oPOM and MAOM fractions were then dried at 60 °C. Analyses for C and N were done on 3 mg samples for fPOM and oPOM using a micro CN analyser (FlashSmart, Thermo Fisher Scientific, USA), while on 100 mg samples for MAOM and bulk using a LECO analyser (LECO Truspec CHN Analyser). The LECO was used for the analyses of the MAOM fraction and the bulk organo-mineral mixture because higher amounts allowed for the detection of N in the MAOM fraction and for a better representation of the heterogeneity of the mixture for the bulk, respectively. Another MAOM sub-sample was burned at 550 °C for 3 h to remove OC, which was then calculated as the difference between total carbon and IC[71].

The recovery of the total C as the sum of the fractions compared to the C measured in the bulk material was overall above 100%. As we excluded an influence of the salts on the weight of the fractions, a problem with the mass recovery and an effect of the analytical device used for the measurements, we attribute the high recoveries we measured to the high heterogeneity of the organo-mineral mixture for which it was difficult to obtain a representative bulk sample.

Phospholipid fatty acid and neutral fatty acid analyses

To analyse the microbial community composition, we carried out a PLFA analysis on freshly collected samples after 120 days. After collection, samples were first frozen at −20 °C prior analyses. The extraction was performed following Frostegård et al.[72] and Bligh et al.[72,73] using a Bligh and Dyer solution for lipid extractions followed by a solid phase extraction using a vacuum concentrator (SpeedVac, Thermo Fisher Scientific, Waltham, USA). PLFAs were then measured using a Gas Chromatograph (GC-MS) (Agilent Technologies, Santa Clara, USA). Samples from treatments with only rock powder did not contain enough microbial biomass to show a sufficient signal in the GC-MS, meaning that values for both bacterial and fungal abundance were not measurable and therefore not accounted for in these treatments. PLFAs were divided into Gram-positive (GP), Gram-negative (GN), Actinomycetes, Anaerobe, Eukaryote and saprophytic Fungi microbial groups and arbuscular mycorrhizal fungi (AMF) were also quantified using the MIDI Sherlock Software v.6.3B with PLFA package v.2.00 (Shimadzu, Kyoto, Japan)[74]. Specific peaks assigned to different microbial groups can be found in Supplementary Table 1. We further calculated the GP:GN and fungal PLFA:bacterial PLFA ratios, as they can be used as an indicator of the type of available C in the system[75] and of the microbial community composition[76], respectively.

Respiration measurements

We measured CO_2 emissions at day 2, 4, 6, 11, 13, 18, 20, 25, 32, 39, 46, 63, 77, 90, 104 and 119 using a Gasera One photoacoustic gas monitor (Gasera, Finland). Gas measurements were always taken 24 h after a watering event. Prior to measurements, microcosms were placed in air-tight jars which were

flushed with a gas with a stable CO_2 concentration for 15 min to ensure a proper flush of the jar and avoid contamination from breathing air. Afterwards, jars were incubated for 40 min and, at the end of the incubation time, gas samples were collected from the headspace of the jars and analysed through the gas analyser. An ambient air sample was always taken in between measurements to prevent contamination between measurements. As CO_2 concentrations did not change over time in the technical control treatments with only rock powder, we used these concentrations as CO_2 background values for further calculations of daily and cumulative emissions. For CO_2 emission analyses, we considered only the five replicates of the treatments which were incubated for the full duration of the experiment (120 days) to avoid potential bias due to removing half of the pots on day 60 and as, during the first 60 days, significant differences in emissions were not found between the two series of destructive replicates. We then calculated the amount of C respired per hour per gram of organo-mineral mixture to further calculate daily and cumulative emissions (Eq. 4).

$$CO_2 - C\left[\frac{\mu g CO_2 - C}{h \cdot g org - \min mix}\right] = \left(\frac{\Delta CO_2 \left[\mu g L^{-1}\right]}{\Delta t [h]} \cdot \frac{V_{hds}[L]}{org - \min mix [g]}\right) \cdot \frac{12}{44}$$

(4)

where $\Delta CO_2/\Delta t$ is the increase in CO_2 over time, V_{hds} is the headspace volume of the jar, org-min mix is the amount of organo-mineral mixture per column, and 12 and 44 are the atomic masses of C and CO_2, respectively. ΔCO_2 was first converted from ppm to g·L^{-1} by diving the concentration by 24.45, which is the conversion factor for an ideal gas at 25° and 1 atm, and multiplied by 10^6 to convert g to μg.

Statistical analyses

All data were tested for normality through visual assessment, the Shapiro–Wilk test and Levene's test. If data were normally distributed, data were analysed using ANOVA followed by a post-hoc Tukey test when the effect was found to be significant ($P < 0.05$), both from the R package "stats"[77]. If data did not meet the assumptions of normality, data were analysed using a non-parametric Kruskal–Wallis test using the R package "stats"[77]. When the effect was found to be significant ($P < 0.05$), we carried out a post-hoc Dunn test using the R package "dunn.test"[78]. When data was analysed for the interaction between treatments and time, first it was transformed using a Aligned Ranked Transformation (ART) using the R package "ARTool"[79] and then a two-way ANOVA was performed, followed by a post-hoc Tukey test when significant differences were found ($P < 0.05$). All data were analysed using Rstudio (version 4.3.1).

Reporting summary

Further information on research design is available in the Nature Portfolio Reporting Summary linked to this article.

Data availability

The datasets generated and analysed during the current study are deposited in the open-access Pangaea data repository with title "Influence of live and dead earthworms on carbon stabilisation and sequestration through mineral weathering" (https://doi.org/10.1594/PANGAEA.984356). For the analyses on organic matter fractions, microbial communities and parameters measured in the leachate, the dataset "Influence of live and dead earthworms on carbon stabilization and sequestration through mineral weathering - Organo-mineral mixture and leachate" (https://doi.org/10.1594/PANGAEA.984355) was used. For the analyses on CO_2 emissions, the dataset "Influence of live and dead earthworms on carbon stabilization and sequestration through mineral weathering - Gas emissions" (https://doi.org/10.1594/PANGAEA.984354) was used.

References

1. United Nations. *Adoption of the Paris Agreement*. U.N. Doc. FCCC/CP/2015/L.9/Rev/1 (United Nations, 2015).
2. Rogelj, J. et al. A new scenario logic for the Paris Agreement long-term temperature goal. *Nature* **573**, 357–363 (2019).
3. Strefler, J. et al. Carbon dioxide removal technologies are not born equal. *Environ. Res. Lett.* **16**, 1–11 (2021).
4. Strefler, J., Amann, T., Bauer, N., Kriegler, E. & Hartmann, J. Potential and costs of carbon dioxide removal by enhanced weathering of rocks. *Environ. Res. Lett.* **13**, 2–10 (2018).
5. Hartmann, J. et al. Enhanced chemical weathering as a geoengineering strategy to reduce atmospheric carbon dioxide, supply nutrients, and mitigate ocean acidification. *Rev. Geophys.* **51**, 113–149 (2013).
6. Hartmann, J., Jansen, N., Dürr, H. H., Kempe, S. & Köhler, P. Global CO2-consumption by chemical weathering: what is the contribution of highly active weathering regions?. *Glob. Planet Change* **69**, 185–194 (2009).
7. Buss, W., Hasemer, H., Sokol, N. W., Rohling, E. J. & Borevitz, J. Applying minerals to soil to draw down atmospheric carbon dioxide through synergistic organic and inorganic pathways. *Commun. Earth Environ.* **5**, 602 (2024).
8. Lei, K. et al. Balancing organic and inorganic carbon dynamics in enhanced rock weathering: implications for carbon sequestration. *Glob. Change Biol.* **31**, e70186 (2025).
9. Sokol, N. W. & Bradford, M. A. Microbial formation of stable soil carbon is more efficient from belowground than aboveground input. *Nat. Geosci.* **12**, 46–53 (2019).
10. Lavallee, J. M., Soong, J. L. & Cotrufo, M. F. Conceptualizing soil organic matter into particulate and mineral-associated forms to address global change in the 21st century. *Glob. Change Biol.* **26**, 261–273 (2020).
11. Buss, W., Hasemer, H., Ferguson, S. & Borevitz, J. Stabilisation of soil organic matter with rock dust partially counteracted by plants. *Glob. Change Biol.* **30**, e17052 (2024).
12. Vicca, S. et al. Is the climate change mitigation effect of enhanced silicate weathering governed by biological processes?. *Glob. Change Biol.* **28**, 711–726 (2022).
13. Vienne, A. et al. Earthworms in an enhanced weathering mesocosm experiment: Effects on soil carbon sequestration, base cation exchange and soil CO2 efflux. *Soil Biol. Biochem.* **199**, 109596 (2024).
14. Vidal, A. et al. The role of earthworms in agronomy: Consensus, novel insights and remaining challenges. in *Advances in Agronomy*, Vol. **181**, 1–78 (Academic Press Inc., 2023).
15. Suzuki, Y., Matsubara, T. & Hoshino, M. Breakdown of mineral grains by earthworms and beetle larvae. *Geoderma* **112**, 131–142 (2003).
16. Needham, S. J., Worden, R. H. & Mcilroy, D. Animal-sediment interactions: the effect of ingestion and excretion by worms on mineralogy. *Biogeosciences* **1** www.biogeosciences.net/bg/1/113/ (2004).
17. Carpenter, D., Hodson, M. E., Eggleton, P. & Kirk, C. Earthworm induced mineral weathering: Preliminary results. *Eur. J. Soil Biol.* **43**, S176–S183 (2007).
18. Liu, D., Lian, B., Wu, C. & Guo, P. A comparative study of gut microbiota profiles of earthworms fed in three different substrates. *Symbiosis* **74**, 21–29 (2018).
19. Liu, D., Lian, B., Wang, B. & Jiang, G. Degradation of potassium rock by earthworms and responses of bacterial communities in its gut and surrounding substrates after being fed with mineral. *PLoS ONE* **6**, e28803 (2011).
20. Vidal, A. et al. Earthworm cast formation and development: A shift from plant litter to mineral associated organic matter. *Front. Environ. Sci.* **7**, 55 (2019).
21. Kögel-Knabner, I. et al. Organo-mineral associations in temperate soils: integrating biology, mineralogy, and organic matter chemistry. *J. Plant Nutr. Soil Sci.* **171**, 61–82 https://doi.org/10.1002/jpln.200700048 (2008).
22. Carpenter, D., Hodson, M. E., Eggleton, P. & Kirk, C. The role of earthworm communities in soil mineral weathering: a field experiment. *Mineral. Mag.* **72**, 33–36 (2008).
23. Schwartzman, D. The geobiology of weathering: a 13th hypothesis (2015).
24. Parmelee, R. W. & Crossley, D. A. Jr Earthworm production and role in the nitrogen cycle of a no-tillage agroecosystem on the Georgia Piedmont. *Pedobiologia* **32**, 5–6 (1988).
25. Lin, J. et al. Earthworms exert long lasting afterlife effects on soil microbial communities. *Geoderma* **420**, 115906 (2022).
26. Kos, M. et al. After-life effects: living and dead invertebrates differentially affect plants and their associated above- and belowground multitrophic communities. *Oikos* **126**, 888–899 (2017).
27. Ribeiro, I. D. A. et al. Use of mineral weathering bacteria to enhance nutrient availability in crops: a review. *Front. Plant Sci.* **11**, 590774 (2020).
28. Calogiuri, T. et al. How earthworms thrive and drive silicate rock weathering in an artificial organo-mineral system. *Appl. Geochem.* **180**, 106271 (2025).
29. Dixon, G. R., & Tilston, E. L. (eds). *Soil Microbiology and Sustainable Crop Production* (Springer Science & Business Media, 2010)
30. Middelburg, J. J., Soetaert, K. & Hagens, M. Ocean alkalinity, buffering and biogeochemical processes. *Rev. Geophys.* **58** https://doi.org/10.1029/2019RG000681 (2020).
31. Amann, T., Hartmann, J., Hellmann, R., Pedrosa, E. T. & Malik, A. Enhanced weathering potentials—the role of in situ CO2 and grain size distribution. *Front. Climate* **4**, 929268 (2022).
32. Aira, M., Pérez-Losada, M. & Domínguez, J. Microbiome dynamics during cast ageing in the earthworm Aporrectodea caliginosa. *Appl. Soil Ecol.* **139**, 56–63 (2019).
33. Aira, M., Lazcano, C., Gómez-Brandón, M. & Domínguez, J. Ageing effects of casts of Aporrectodea caliginosa on soil microbial community structure and activity. *Appl. Soil Ecol.* **46**, 143–146 (2010).
34. Kellerová, A., Angst, G. & Jílková, V. Earthworms facilitate stabilization of both more-available maize biomass and more-recalcitrant maize biochar on mineral particles in an agricultural soil. *Soil Biol. Biochem.* **189**, 109278 (2024).
35. Zhang, W. et al. Earthworms facilitate carbon sequestration through unequal amplification of carbon stabilization compared with mineralization. *Nat. Commun.* **4**, 2576 (2013).
36. Van Groenigen, J. W. et al. How fertile are earthworm casts? A meta-analysis. *Geoderma* **338**, 525–535 https://doi.org/10.1016/j.geoderma.2018.11.001 (2019).
37. Angst, G. et al. Earthworms act as biochemical reactors to convert labile plant compounds into stabilized soil microbial necromass. *Commun. Biol.* **2**, 441 (2019).
38. Irshad, S. & Frouz, J. How the effect of earthworms on soil organic matter mineralization and stabilization is affected by litter quality and stage of soil development. *Biogeochemistry* https://doi.org/10.1007/s10533-024-01182-8. (2024)
39. Zi, Y. et al. Let's get functional: Relationship between earthworm traits and physicochemical cast properties. *Soil Biol. Biochem.* **207**, 109809 (2025).
40. Amadou, I. et al. Interactions between earthworm species and soil type influence the porosity of earthworm casts. *Soil Biol. Biochem.* **203**, 109739 (2025).
41. Song, C. et al. Land use determines the composition and stability of organic carbon in earthworm casts under tropical conditions. *Soil Biol. Biochem.* **190**, 109291 (2024).
42. Fanin, N., Hättenschwiler, S. & Fromin, N. Litter fingerprint on microbial biomass, activity, and community structure in the underlying soil. *Plant Soil* **379**, 79–91 (2014).

43. Kramer, C. & Gleixner, G. Soil organic matter in soil depth profiles: Distinct carbon preferences of microbial groups during carbon transformation. *Soil Biol. Biochem.* **40**, 425–433 (2008).

44. Sokol, N. W. et al. Global distribution, formation and fate of mineral-associated soil organic matter under a changing climate: A trait-based perspective. *Funct. Ecol.* **36**, 1411–1429 https://doi.org/10.1111/1365-2435.14040 (2022).

45. Sel, A. & Binal, A. Does bacterial weathering play a significant role in rock weathering? *Environ Earth Sci.* **80** (2021).

46. Liang, C., Amelung, W., Lehmann, J. & Kästner, M. Quantitative assessment of microbial necromass contribution to soil organic matter. *Glob. Change Biol.* **25**, 3578–3590 (2019).

47. Wang, B., An, S., Liang, C., Liu, Y. & Kuzyakov, Y. Microbial necromass as the source of soil organic carbon in global ecosystems. *Soil Biol. Biochem.* **162**, 108422 (2021).

48. Angst, G. et al. Stabilized microbial necromass in soil is more strongly coupled with microbial diversity than the bioavailability of plant inputs. *Soil Biol. Biochem.* **190**, 109323 (2024).

49. Cotrufo, M. F., Wallenstein, M. D., Boot, C. M., Denef, K. & Paul, E. The Microbial Efficiency-Matrix Stabilization (MEMS) framework integrates plant litter decomposition with soil organic matter stabilization: Do labile plant inputs form stable soil organic matter?. *Glob. Change Biol.* **19**, 988–995 (2013).

50. Whalen, J. K., Parmelee, R. W., McCartney, D. A. & Vanarsdale, J. L. Movement of N from decomposing earthworm tissue to soil, microbial and plant N pools. *Soil Biol. Biochem.* **31**, 487–492 (1999).

51. Drever, J. I. *The Geochemistry of Natural Waters* (Prentice Hall, 1988).

52. Hupe, A. et al. Get on your boots: estimating root biomass and rhizodeposition of peas under field conditions reveals the necessity of field experiments. *Plant Soil* **443**, 449–462 (2019).

53. West, A. J., Galy, A. & Bickle, M. Tectonic and climatic controls on silicate weathering. *Earth Planet Sci. Lett.* **235**, 211–228 (2005).

54. White, A. F. & Buss, H. L. Natural weathering rates of silicate minerals. in *Treatise on Geochemistry: Second Edition* Vol. **7**, 115–155 (Elsevier Inc., 2013).

55. Calogiuri, T. et al. Design and construction of an experimental setup to enhance mineral weathering through the activity of soil organisms. *J. Vis. Exp.* **201**, e65563 (2023).

56. Bouché, M. B. Strategies lombriciennes. *Ecol. Bull.* **25**, 122–132 (1977).

57. Uroz, S., Calvaruso, C., Turpault, M. P. & Frey-Klett, P. Mineral weathering by bacteria: ecology, actors and mechanisms. *Trends Microbiol.* **17**, 378–387 (2009).

58. Georgiadis, A., Marhan, S., Lattacher, A., Mäder, P. & Rennert, T. Do earthworms affect the fractionation of silicon in soil?. *Pedobiologia* **75**, 1–7 (2019).

59. Dalby, P. R., Baker, G. H. & Smith, S. E. "Filter paper method" to remove soil from earthworm intestines and to standardise the water content of earthworm tissue. *Soil Biol. Biochem.* **28**, 685–687 (1996).

60. Pulleman, M. M., Six, J., Uyl, A., Marinissen, J. C. Y. & Jongmans, A. G. Earthworms and management affect organic matter incorporation and microaggregate formation in agricultural soils. *Appl. Soil Ecol.* **29**, 1–15 (2005).

61. Perreault, J. M. & Whalen, J. K. Earthworm burrowing in laboratory microcosms as influenced by soil temperature and moisture. *Pedobiologia* **50**, 397–403 (2006).

62. Capowiez, Y., Sammartino, S., Keller, T. & Bottinelli, N. Decreased burrowing activity of endogeic earthworms and effects on water infiltration in response to an increase in soil bulk density. *Pedobiologia* **85–86**, 150728 (2021).

63. De Troyer, I., Amery, F., Van Moorleghem, C., Smolders, E. & Merckx, R. Tracing the source and fate of dissolved organic matter in soil after incorporation of a 13C labelled residue: A batch incubation study. *Soil Biol. Biochem.* **43**, 513–519 (2011).

64. Anda, M., Shamshuddin, J. & Fauziah, C. I. Improving chemical properties of a highly weathered soil using finely ground basalt rocks. *Catena* **124**, 147–161 (2015).

65. Amann, T. & Hartmann, J. Carbon accounting for enhanced weathering. *Front. Climate* **4**, 849948 (2022).

66. Amann, T., Hartmann, J., Hellmann, R., Pedrosa, E. T. & Malik, A. Enhanced weathering potentials—the role of in situ CO2 and grain size distribution. *Front. Climate* **4**, 929268 (2022).

67. Vienne, A. et al Enhanced weathering using basalt rock powder: carbon sequestration, co-benefits and risks in a mesocosm study with Solanum tuberosum. *Front. Climate* **72**. https://doi.org/10.3389/fclim.2022.869456. (2022)

68. Campos-M, M. & Campos-C, R. Applications of quartering method in soils and foods. *Int. J. Eng. Res. Appl.* **7**, 35–39 (2017).

69. Plaza, C., Giannetta, B., Benavente, I., Vischetti, C. & Zaccone, C. Density-based fractionation of soil organic matter: effects of heavy liquid and heavy fraction washing. *Sci. Rep.* **9**, 10146 (2019).

70. Cerli, C., Celi, L., Kalbitz, K., Guggenberger, G. & Kaiser, K. Separation of light and heavy organic matter fractions in soil - Testing for proper density cut-off and dispersion level. *Geoderma* **170**, 403–416 (2012).

71. Koorneef, G. J. et al. Quantifying organic carbon in particulate and mineral-associated fractions of calcareous soils – A method comparison. *Geoderma* **436**, 116558 (2023).

72. Frostegård, Å, Tunlid, A. & Bååth, E. Microbial biomass measured as total lipid phosphate in soils of different organic content. *J. Microbiol. Methods* **14**, 151–163 (1991).

73. Bligh, E. G. & Dyer, W. J. A rapid method of total lipid extraction and purification. *Can. J. Biochem. Physiol.* **37**, 911–917 (1959).

74. Buyer, J. S. & Sasser, M. High throughput phospholipid fatty acid analysis of soils. *Appl. Soil Ecology* **61**, 127–130 (2012).

75. Fanin, N. et al. The ratio of Gram-positive to Gram-negative bacterial PLFA markers as an indicator of carbon availability in organic soils. *Soil Biol. Biochem.* **128**, 111–114 (2019).

76. Onica, B. M., Stoian, V. & Vidican, R. The Importance Of Fungal/Bacterial Ratio In Grasslands. *Rom. J. Grassl. Forage Crops* **16**, 33 (2017).

77. R Core Team. *R: A language and environment for statistical computing.* R Foundation for Statistical Computing, Vienna, Austria. https://www.R-project.org/. (2023)

78. Dinno, A. _dunn.test: Dunn's Test of Multiple Comparisons Using Rank Sums_. R package version 1.3.5, https://CRAN.R-project.org/package=dunn.test (2017).

79. Kay, M., Elkin, L. A., Higgins, J. J. & Wobbrock, J. O. ARTool: aligned rank transform. CRAN: Contributed Packages (2014).

Acknowledgements

Author contributions

T.C. designed and built the experimental set-up, carried out the experiment, data collection and analyses, and wrote the manuscript; M.H. designed and supervised the experiment and wrote the manuscript; J.W.G. supervised the experiment and wrote the manuscript; F.W. provided the ^{13}C labelled litter, reviewed and edited the manuscript; R.P.P. contributed to data interpretation, reviewed and edited the manuscript; L.R. contributed to

Competing interests

The authors declare no competing interests.

Additional information

Supplementary information The online version contains supplementary material available at https://doi.org/10.1038/s43247-025-02766-4.

Correspondence and requests for materials should be addressed to Tullia Calogiuri.

Peer review information *Communications Earth and Environment* thanks Dima Chen and the other, anonymous, reviewer(s) for their contribution to the peer review of this work. Primary Handling Editors: Leiyi Chen and Mengjie Wang. [A peer review file is available].

Reprints and permissions information is available at http://www.nature.com/reprints

Publisher's note Springer Nature remains neutral with regard to jurisdictional claims in published maps and institutional affiliations.